

1 Predictive Prosthetic Socket Design: Part 2 2 – generating person-specific candidate 3 designs using multi-objective Genetic 4 Algorithms

5 J.W. Steer, P.A. Grudniewski, M. Browne, P.R. Worsley, A.J. Sobey, A.S. Dickinson

6 J.W. Steer: joshua.steer@soton.ac.uk; ORCID 0000-0002-6288-1347

7 P.A. Grudniewski: pag1c15@soton.ac.uk; ORCID 0000-0003-0635-3125

8 M. Browne: doctor@soton.ac.uk; ORCID 0000-0001-5184-050X

9 P.R. Worsley: p.r.worsley@soton.ac.uk; ORCID 0000-0003-0145-5042

10 A.J. Sobey: ajs502@soton.ac.uk; ORCID 0000-0001-6880-8338

11 A.S. Dickinson: alex.dickinson@soton.ac.uk; ORCID 0000-0002-9647-1944

12 Abstract

13 In post-amputation rehabilitation, a common goal is to return to ambulation using a prosthetic limb,
14 suspended by a customised socket. Prosthetic socket design aims to optimise load transfer between
15 the residual limb and mechanical limb, by customisation to the user. This is a time consuming
16 process and with the increase in people requiring these prosthetics it is vital that these personalised
17 devices can be produced rapidly whilst maintaining excellent fit, to maximise function and comfort.

18 Prosthetic sockets are designed by capturing the residual limb's shape, and applying a series of
19 geometrical modifications, called rectifications. Expert knowledge is required to achieve a
20 comfortable fit in this iterative process. A variety of rectifications can be made, grouped into
21 established strategies (e.g. in transtibial sockets: patellar tendon bearing (PTB) and total surface
22 bearing (TSB)), creating a complex design space. To date, adoption of advanced engineering
23 solutions to support fitting has been limited. One method is numerical optimisation, which allows
24 the designer a number of likely candidate solutions to start the design process. Numerical
25 optimisation is commonly used in many industries but not prevalent in the design of prosthetic
26 sockets.

27 This paper therefore presents candidate shape optimisation methods which might benefit the
28 prosthetist and the limb user, by blending the state-of-the-art from prosthetic mechanical design,
29 surrogate modelling and evolutionary computation. The result of the analysis is a series of prosthetic
30 socket designs that preferentially load and unload the pressure tolerant and intolerant regions of the
31 residual limb. This spectrum is bounded by the general forms of the PTB and TSB designs, with a
32 series of variations in between that represent a compromise between these accepted approaches.
33 This results in a difference in pressure of up to 31 kPa over the fibula head and 14 kPa over the
34 residuum tip.

35 The presented methods would allow a trained prosthetist to rapidly assess these likely candidates
36 and then to make final detailed modifications and fine-tuning. Importantly, insights gained about the
37 design should be seen as a compliment, not a replacement, for the prosthetist's skill and experience.
38 We propose instead that this method might reduce the time spent on the early stages of socket
39 design, and allow prosthetists to focus on the most skilled and creative tasks of fine-tuning the
40 design, in face-to-face consultation with their client.

41 Requirement of automation in design of prosthetics

42 Approximately 40 million people globally require access to prosthetic or orthotic services [2].
43 Prosthesis-human interface design aims to maximise comfort and functionality for people with
44 amputations, towards ambulatory rehabilitation. This is commonly provided through a prosthetic
45 socket, which is designed through geometric modifications to the captured shape of the residual
46 limb, known as rectifications, to create a desired pattern of load transfer. This is currently an
47 iterative process performed by a highly skilled prosthetist, who manages the residuum's changing
48 size, shape, soft tissue healing and biomechanical adaptation. Indeed, due to these factors, the
49 development of a definitive socket takes a considerable period of time. Prosthetic limb users require
50 life-long access to prosthetics services, and in the UK the annual cost of prosthesis provision and
51 care is over £2,800 per patient [3]. This includes the replacement of prosthetic limb components
52 typically every two to five years. Skilled prosthetists take many years to train to a high standard and
53 often prosthetic users develop relationships with their preferred clinician to maintain socket
54 comfort. However, there are limited numbers of these highly skilled individuals and practice
55 efficiencies are required in the face of growing clinical demand. Researchers have considered
56 mechanisms for employing quantitative prediction in the socket design process [4, 5]], although at
57 present these work to a single design target for a single individual, and have not entered
58 conventional clinical use.

59 In Part One of this study [1], a Kriging-based surrogate model was generated for a parametric FE
60 model of a population-based transtibial residual limb and accompanying total surface bearing (TSB)
61 socket design. This enabled the prediction of biomechanical relationships between the residual limb
62 morphology and prosthetic socket design, while reducing the computational cost of each new
63 prediction by six orders of magnitudes (1.6 ms vs 30 minutes). The simplified total surface bearing
64 socket design was defined parametrically from the limb's neutral shape, by reducing the cross-
65 sectional area along its length with three points at the proximal, mid and distal regions of the socket.
66 However, within a clinical setting, the socket design process is substantially more nuanced. There are
67 several different design philosophies, all with different intended residual limb load transfer
68 mechanisms. The classic patella tendon bearing (PTB) socket design was developed in 1957, and is
69 still commonly used in-clinic today [6]. This socket design aims to apply pressure over load-tolerant
70 areas of the limb such as the patella tendon, and off-load pressure sensitive regions such as the
71 anterior tibia, fibula head and residuum tip. Other sockets include the Kondylen-Bettung Münster
72 (KBM) which provides supracondylar suspension in addition to features consistent with the patella
73 tendon bearing design [7], and hydrostatic sockets [8] such as the PCAST system [9–13] which uses a
74 pressurised fluid as a medium to form the shape of the socket with the aim of achieving minimal
75 residuum surface pressure gradients with less manual intervention. More recently total surface
76 bearing sockets, which were proposed in 1987, are used to generate near-total contact in between
77 the residual limb and the socket [14, 15]. In theory, this should maximise the contact area between
78 the residual limb and prosthetic socket and the uniformity of pressure across the surface of the
79 residual limb, thereby minimising potentially harmful pressure gradients [15].

80 Despite the fundamental differences in the load distribution between these socket designs, they can
81 potentially all deliver satisfactory outcomes for prosthesis users [16]. There is substantial research
82 into quantifying the biomechanical differences between these socket designs, which is
83 comprehensively reviewed by Safari and Meier in 2015 [17]. Their systematic review concluded that
84 “the included studies only had low to moderate methodological rigour”, thus demonstrating the
85 difficulties in defining biomechanical guidelines for the highly dynamic environment of the residual
86 limb – prosthetic socket system, or selection of the preferred socket type for a particular individual

87 or situation. One possible reason for the difficulty in establishing the definitive guidelines of these
88 different socket types is that they are defined primarily by design intent, rather than quantitative
89 rules. This effect has been illustrated for a simple total surface bearing socket using parametric FEA
90 [1], and it is almost certain the within-type variability would be increased for more complex designs.
91 We propose that there is a large potential to enhance the evidence base behind this clinical
92 challenge, allowing prosthetists to develop, critique and share their own expertise and decision
93 making, making more effective use of their valuable design and consultation time. A key and
94 relatively unexplored possibility is to apply automated search algorithms to explore designs prior to
95 optimisation for the individual.

96 Optimisation algorithms are common in many areas of engineering to reduce design time. They are
97 commonly used as concept design methods, providing an initial product which engineers can use as
98 a starting point and to increase the proportion of their time spent on creatively solving complex
99 problems. In addition, they provide a visualisation for how these changes will affect the final
100 product's performance, allowing a greater understanding of the design space which can be put to
101 use in the more detailed stages of the process. A choice of potential candidate designs can be
102 provided to the decision maker, which weight the objectives differently, for example putting more
103 load on the residuum tip and removing it from the fibular head, and therefore give a range of
104 performances. This requires algorithms capable of multi-objective optimisation that provide a rapid
105 convergence on the global optimum while retaining a high diversity of the search, to ensure that the
106 entire search space is investigated and that the focus is not upon local optima. Many methodologies
107 have been developed and state-of-the-art research focuses on improvements in diversity or
108 convergence.

109 This paper employs optimisation algorithms to generate personalised 'candidate' prosthetic socket
110 designs for the first time. This is applied to the transtibial case, which is the most common major
111 lower limb amputation and where most clinical success has been achieved with associated CAD/CAM
112 socket design and fabrication tools. Different design problems require different optimisation
113 processes. The aim is therefore to determine appropriate methods for the automated application of
114 candidate socket rectifications, collating the state-of-the-art in biomechanical analysis of prosthesis-
115 limb interfaces, surrogate modelling and optimisation. Genetic Algorithms are chosen due to their
116 ability to effectively search large and complex design spaces, which is the problem presented by the
117 continually variable distribution of possible limb-socket shape rectifications. These methods rely on
118 thousands of function calls, and using FE models would not be feasible beyond single cases due to
119 the time required for each simulation. However, by leveraging the speed increases of the surrogate
120 model [1], it becomes technically feasible to perform automated socket optimisation based upon
121 structural analysis of the limb-prosthesis system. This provides the motivation for the current study,
122 to perform a first-of-kind, subject-specific, multi-objective design optimisation of the prosthetic
123 socket using the previously reported surrogate model. The result will be a series of personalised
124 'candidate' transtibial prosthetic socket designs, to which the prosthetist would add local
125 modifications based upon their knowledge and conventional patient consultation. Finally, equipped
126 with these results, a prosthetist would then further refine these concepts to achieve a desired
127 pattern of prosthesis-limb load transfer, by using these designs to augment their experience-based
128 decision making.

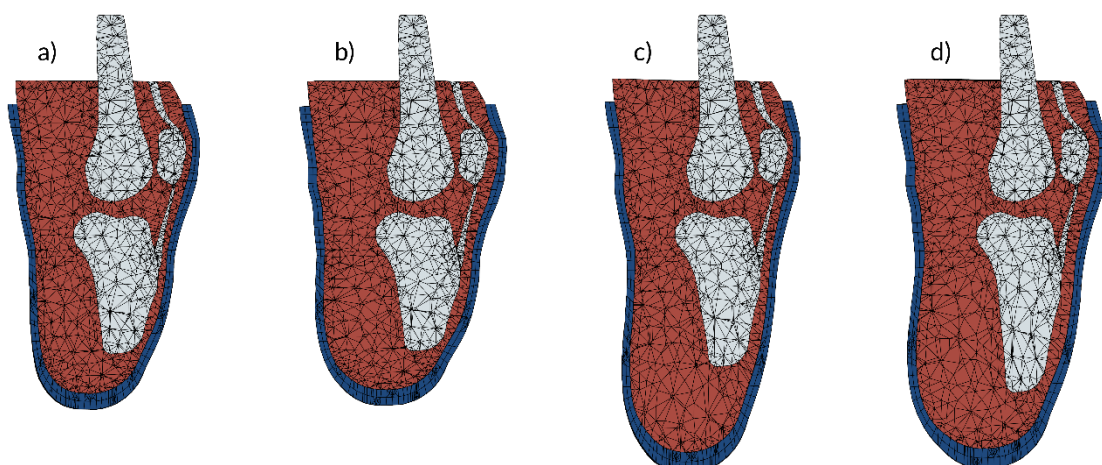
129 Optimisation of transtibial prosthetic sockets

130 Population-based surrogate model

131 A detailed description of the population-based surrogate model is found in Part I of this paper [1]. In
 132 short, a generic residual limb was generated by producing a volume mesh from an MRI scan and
 133 imposing radial basis function mesh morphing to apply parametric variation in residuum length and
 134 profile (conical to bulbous) obtained from principal modes of variation from a population of 3D
 135 surface scans. These were varied by $\pm 1 \sigma$ (standard deviation) about the mean length and profile in
 136 the statistical shape model (SSM). Furthermore, internal parametric variation of the relative tibia
 137 length (i.e. distal soft tissue coverage) from -15% to +30% of the tibia length from the MRI scan, and
 138 soft tissue material properties between stiff, flaccid muscle and contracted muscle [18–20] were
 139 applied. The soft tissue was assigned a neo-Hookean material to capture the non-linear behaviour of
 140 the soft tissue. The present surrogate model implementation investigates the effects of socket
 141 design variation for four synthetic ‘virtual’ people sequentially by selecting exemplar values for the
 142 model’s residuum variability parameters (Table 1, Figure 1). These cases were chosen as being close
 143 to the models’ population extremes whilst remaining within the bounding box of the sampling plan,
 144 to avoid extrapolating beyond the surrogate. These meshes were imported into the finite element
 145 solver (ABAQUS 6.14, Dassault Systèmes, Vélizy-Villacoublay, France). The socket was donned under
 146 displacement control and loaded uniaxially to 400N to simulate a two-leg stance. The resultant
 147 pressure and soft tissue strain outputs from 75 simulations were used to construct a kriging
 148 surrogate model for each virtual person, enabling a function call to be made in ~2ms.

149 *Table 1: Parameters of the four cases extracted from the parametric residual limb model. Soft tissue initial modulus*
 150 *corresponds to the initial stiffness of the applied neo-Hookean hyperelastic material model.*

| Virtual Person | Residuum length, ν_1 | Residuum Profile, ν_2 | Tibia Length, ν_3 | Soft tissue initial modulus, ν_4 |
|----------------|--------------------------|---------------------------|-----------------------|--------------------------------------|
| A | -0.8σ (Short) | -0.8σ (Bulbous) | +20% (Long) | 40 kPa (Soft) |
| B | -0.8σ (Short) | $+0.8 \sigma$ (Conical) | -5% (Short) | 50 kPa (Stiff) |
| C | $\mp 0.8 \sigma$ (Long) | -0.8σ (Bulbous) | +20% (Long) | 40 kPa (Soft) |
| D | $\mp 0.8 \sigma$ (Long) | $+0.8 \sigma$ (Conical) | -5% (Short) | 50 kPa (Stiff) |



152
 153 *Figure 1: Sagittal sections through equivalent residuum FE models for the four virtual people. Blue indicates the liner, red*
 154 *the soft tissue, and grey the bones. The prosthetic socket is not shown.*

156 **Parametric socket design**

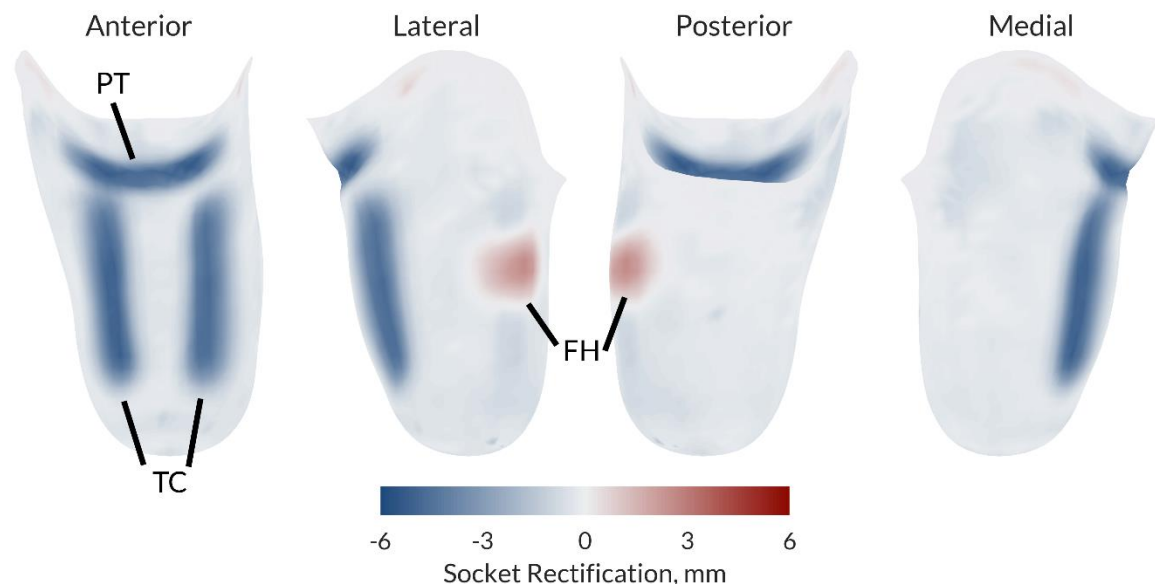
157 In the preceding work [1], a simplified, 3-parameter total surface bearing socket design was used.
158 This model enabled control of the socket press-fit by reducing its cross sectional area through a B-
159 spline function with proximal, mid and distal control points. The three variables were constrained
160 between -1% and 3% by cross-sectional area reduction [Part 1]. The present study's socket design
161 was extended to include the localised rectifications observed in patella tendon bearing sockets.
162 Control points were generated over the fibula head, patella tendon and either side of the tibial crest
163 ([Figure 2](#)). These localised rectifications were applied using the same radial basis function mesh
164 morphing algorithm detailed in Part I by radially displacing the control points between 0 - 6 mm.

165 *Table 2: Parameters and limits of the parametric socket design*

| Socket rectification variable name | Lower bound | Upper bound |
|------------------------------------|-------------|-------------|
| Proximal press fit | -2 % | +6% |
| Mid press fit | -2 % | +6% |
| Distal press fit | -2 % | +6% |
| Patella tendon bar | 0 mm | 6 mm |
| Fibula head relief | 0 mm | 6 mm |
| Tibial crest | 0 mm | 6 mm |

166

167



168

169 *Figure 2: Rectification maps of the patella tendon bearing socket design at the maximum values of patella tendon bar (PTB),*
170 *fibula head (FH) relief and tibial crest (TC) rectifications. The figure demonstrates the resulting socket shape change once*
171 *the control nodes have been displaced, and explains the convention directions of each rectification type (FH vs. PT & TC).*

172 **Optimisation via genetic algorithms**

173 Genetic algorithms (GA) are population-based multi-objective solvers inspired by the principles of
174 Darwinian evolution [21]. In a simple Genetic Algorithm a set of potential solutions, called
175 individuals, reproduce via an evolutionary-like process. Each individual contains set of decision
176 variables, called chromosomes, with an initial population with variables that are usually assigned
177 randomly. The fitness of each individual can be evaluated according to some predefined objectives.
178 After this step individuals are then chosen for reproduction and, according to the principles of

179 natural selection, the fitter individuals have significantly higher chances of reproducing than those
180 with a low fitness. Offspring are generated from the selected parents using crossover and mutation
181 processes. During crossover the chromosomes of the offspring are produced by mixing the genes of
182 the parents, providing convergence and diversity. In the mutation step the offspring's genes have a
183 small chance to be randomly modified, improving the population diversity. Finally, the old
184 population becomes extinct and is replaced by the new generation, with the new generation being
185 fitter, on average, than the parent generation. This process continues until the predefined
186 termination condition is met, often specified as a maximum number of objective functions calls or
187 total calculation time.

188 Many competing genetic algorithms have been developed, each introducing novel mechanisms to
189 increase the convergence rates and diversity of the search. In the current state-of-the-art of GAs
190 there is particular emphasis on specialist-solvers. According to the "no free lunch" theorem [22], a
191 specialist-solver exhibits high performance on a narrow set of problems but its performance will
192 rapidly decline when outside of this set. Therefore, a suitable methodology has to be selected with
193 respect to the particular problem's characteristics in order to avoid poor performance. The
194 optimisation problem characteristics and their difficulty are defined by the topology of the search
195 and objective spaces, number of local optima and the applied constraints. If the problem
196 characteristics are not known then more than one GA methodology should be applied as their
197 performance can differ drastically. This will provide more reliable results and allow an evaluation of
198 the problem's difficulty and its dominant characteristics [23]. In the case presented in this paper, no
199 knowledge about the characteristic of the problem are available *a priori*, except that no constraints
200 are used. However, this is not sufficient to choose a single properly adjusted optimiser. Therefore, 5
201 different Genetic Algorithms are compared: NSGA-II as the most commonly utilised Genetic
202 Algorithm which retains a high diversity of search and has had much success in the applied literature
203 [24]; MOEA/D as the most proficient algorithm for unconstrained problems [25]; MTS as an
204 aggregation of a Genetic Algorithm and a local-search method which provides improved
205 convergence [26]; cMLSGA and HEIA as the general-type GAs that exhibit high performance across
206 wide range of problem types and therefore higher robustness [27, 28]. HEIA is more dominant in
207 scenarios where convergence is more important and cMLSGA provides a higher diversity of search.
208 The detailed principles of working and parameter settings of each methodology can be found in their
209 respective publications¹. All the tests are performed over 30 separate runs, with 50,000 fitness
210 function evaluations as a termination criterion. Multiple runs must be performed in order to assure
211 the robustness of the method and the best likelihood of identifying the true Pareto Front. Different
212 population sizes have been tested and 600 individuals is utilised as the best for NSGA-II, MTS,
213 MOEA/D and HEIA, while cMLSGA utilises 1800 as it requires significantly higher population sizes
214 [29].

215 The socket design process presented in our prior work [1] can be framed as a formal engineering
216 design optimisation problem. In this case the individual socket rectifications function as design
217 parameters across a multi-dimensional input space, and the resultant pressure and soft tissue strain
218 fields are formulated as the objective functions. The locations across the limb for the objective
219 functions were selected because they are known to be load-intolerant [6]. It was predicted that the
220 introduction of a peripheral press-fit around the main body of the residuum will allow load transfer
221 through the longitudinal shear forces and thus reduce the residuum tip pressure, at the expense of
222 pressure concentrations over the bony prominences of the tibial tuberosity and fibula head. Four
223 state variables were defined: the pressure over the residuum tip (f_1), the tibial tuberosity (f_2), the

¹ Source codes for all methodologies can be found at: <https://bitbucket.org/Pag1c18/cmlsga>

224 fibula head (f_3), and the soft tissue strain around the distal tibia (f_4). These model outputs can be
225 described as competing fitness functions, indicating proximal and distal loading, defined as $FF1 =$
226 $f_1 + f_4$ and $FF2 = f_2 + f_3$. These were evaluated using the surrogate model developed previously
227 [1] for the four synthetic people defined in [Table 1](#).

228 One of the issues with multi-objective optimisation is the comparison of the results obtained by
229 different methods. The visual comparison is limited, only providing useful information when the
230 performance of two solvers differs drastically. Otherwise the points will overlap making objective
231 comparison near impossible. Therefore, multiple quality indicators have been developed [30]. Most
232 of them are able to indicate the performance in both convergence and diversity of the solutions.
233 However, each of them have certain drawbacks or biases and it is common practice to utilise more
234 than one indicator [30]. In this paper the Inverted Generational Distance (IGD) and Hyper Volume
235 (HV) were chosen as indicators. IGD measures the average Euclidean distance between each point in
236 a real Pareto Optimal Front (POF) and the closest solution in the obtained set. Lower values indicate
237 better convergence and uniformity of the points, and are calculated according to eq. 1:

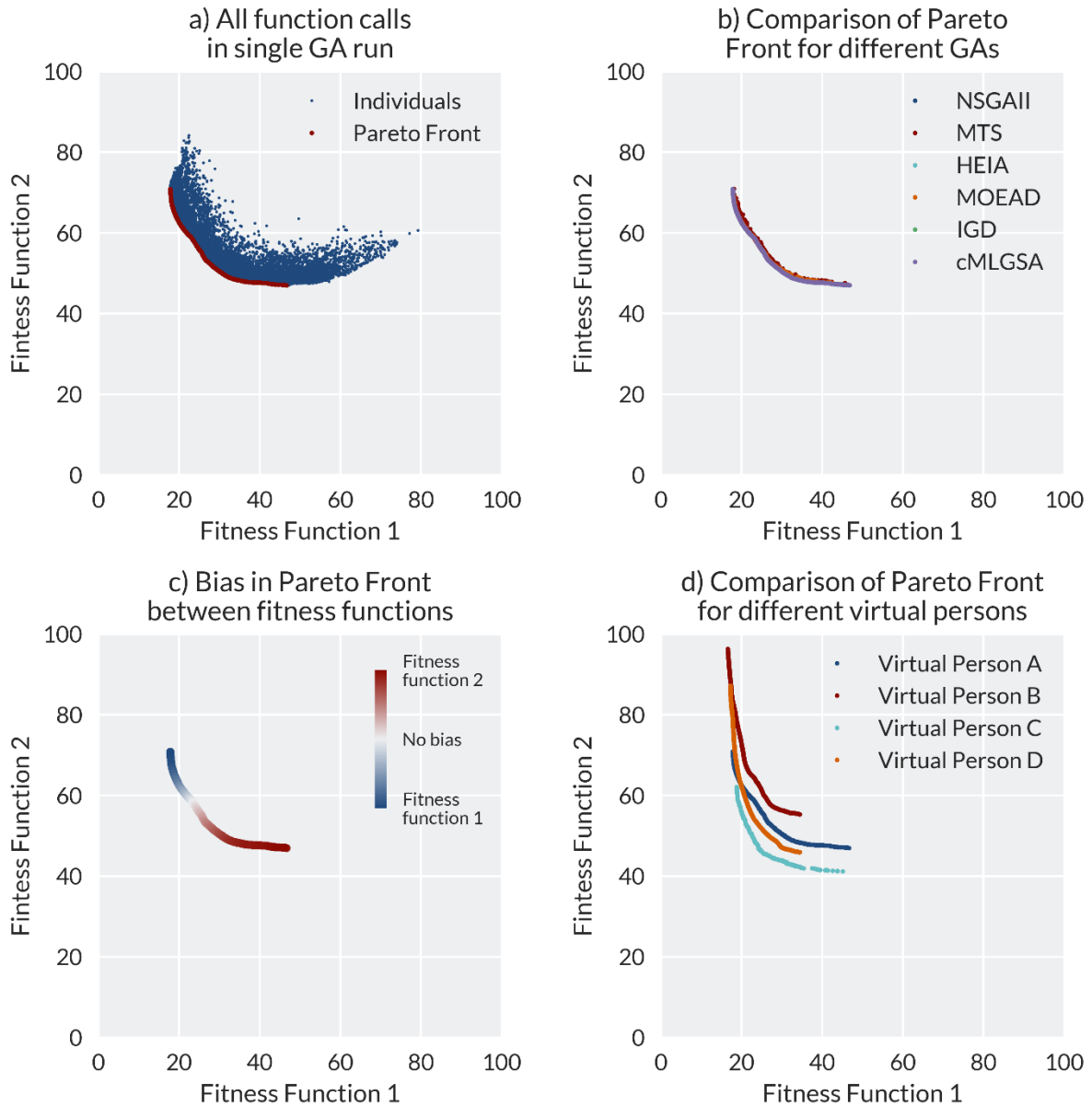
$$238 IGD(A, P^*) = \frac{\sum_{v \in P^*} d(v, A)}{|P^*|},$$

239 where P^* is a set of uniformly distributed points along the true PF, A is the approximate set to the
240 POF, which is being evaluated and $d(v, A)$ is the minimum Euclidean distance between the point v
241 and points in A .

242 However, this IGD shows poor performance in determining the diversity of a population when the
243 Pareto Front population is small. HV is calculated as the volume of an objective space between a
244 predefined reference point and the obtained solutions where higher values are preferred [30]. This
245 indicator has a stronger focus on the diversity and boundary points. Most indicators require a
246 predefined reference Pareto Optimal Front that illustrates the ideal set of solutions. However, in
247 cases where the optimal answer is not known the utilisation of these indicators can be problematic.
248 A solution is to calculate a reference Pareto Optimal Front using the non-dominated selection of
249 Pareto Optimal Fronts achieved by every algorithm when performing multiple runs, or performing a
250 few test runs with significantly higher numbers of iterations than that utilised for comparison [23]. In
251 this paper both are applied, and a combined non-dominated front obtained by brute force from all 6
252 Genetic Algorithms after 300,000 fitness function evaluations was used to determine the success of
253 the algorithm.

254 [Results](#)

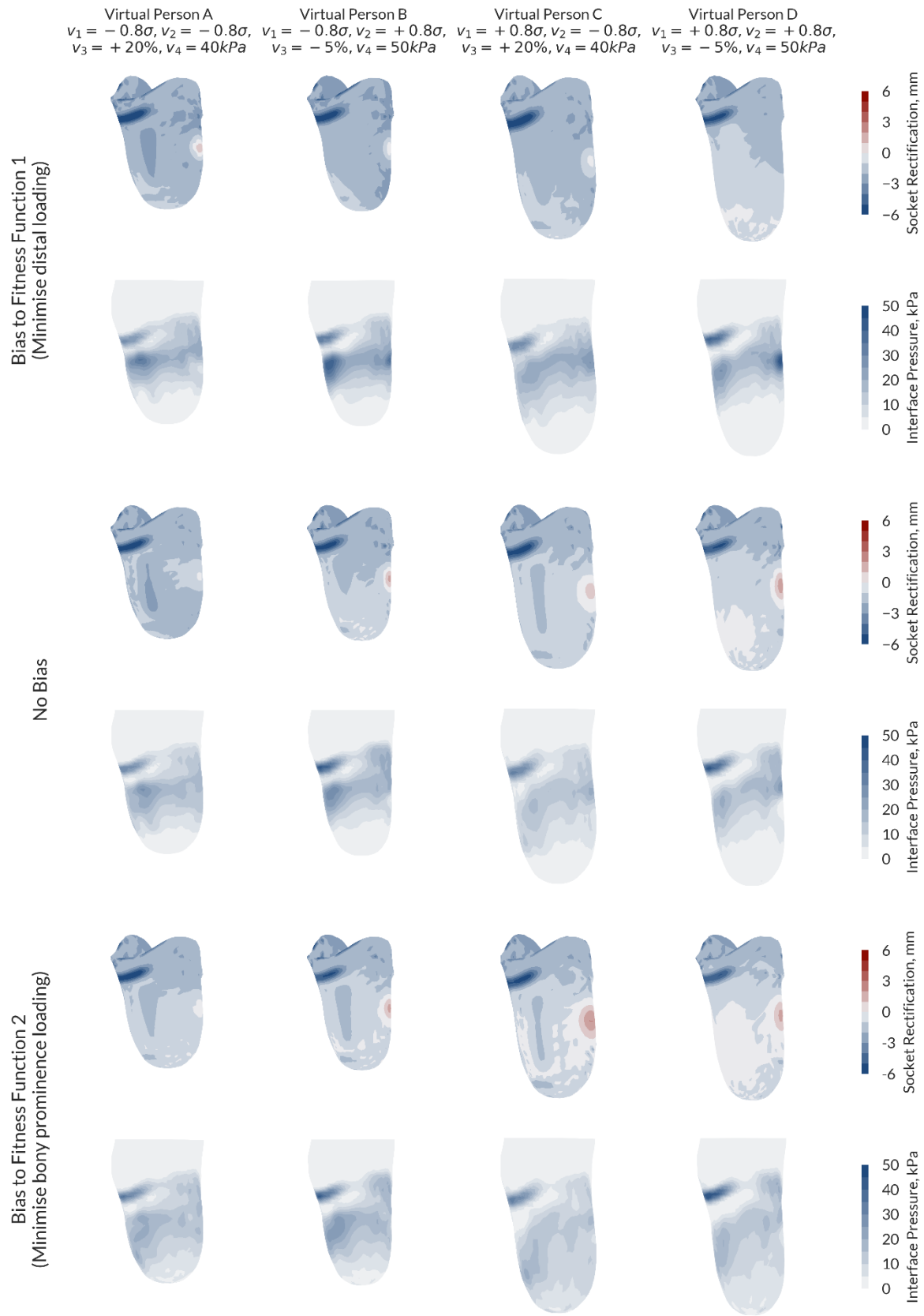
255 A single Genetic Algorithm run with a maximum of 50,000 function calls was computed in
256 approximately 30 minutes, where [Figure 3a](#) shows the individuals evaluated over this lifetime and
257 the final Pareto Front. Comparing the different genetic algorithms, it was observed that the shape of
258 the Pareto Optimal Fronts remains consistent. Therefore, visual comparison only shows that all of
259 the methodologies exhibit similar performance and it is not possible to unanimously choose the best
260 methodology ([Figure 3b](#)). The bias between Fitness Functions FF1 and FF2 along the normalised
261 Pareto Optimal Front is visualised in [Figure 3c](#). The reason the no-bias point is not in the middle of
262 the front is due to the longer 'tail' when minimisation is biased towards FF2 (minimising proximal
263 bony prominence loading), compared with bias towards FF1 (minimising distal tip loading). It was
264 also observed that while the minima of FF1 for all individuals plateaued at just below 20 (unitless),
265 the minima of FF2 were different for all of the virtual people ([Figure 3d](#)). The minima of the short,
266 conical limb of person B and the long, bulbous limb of person C plateaued at $FF2 = 55$ kPa and 40 kPa
267 respectively.



268

269 *Figure 3: Analysis of the Pareto fronts from the multi-objective optimisation. a) Individuals from a single run of the HEIA*
 270 *optimisation for Person A, with all individuals plotted in blue and Pareto front in red. b) Comparison of the generated PFs*
 271 *for the six different GAs tested on Person A. c) Bias along the Pareto front between the two fitness functions, with 'no bias'*
 272 *defined as the minimum distance from the origin to the normalised Pareto Optimal Front, with blue indicating bias towards*
 273 *FF1 and red towards FF2. d) Comparison of the Pareto Fronts for the four different People when using HEIA*

274 From visualisation of the sockets at either end of the Pareto Front, as well as the neutral case,
 275 consistencies in design emerged across the four people (Figure 4). When the optimiser was biased
 276 towards FF1 (minimising tip loading), designs of higher press fit which off-loaded the residuum tip
 277 emerged from the Genetic Algorithm. For person B (Figure 4b) and person D (Figure 4d) pressure
 278 hotspots were generated where there was little soft tissue coverage over the proximal bony
 279 prominences. When the model was biased towards FF2, sockets with higher fibula head relief
 280 evolved in order to off-load over this region.



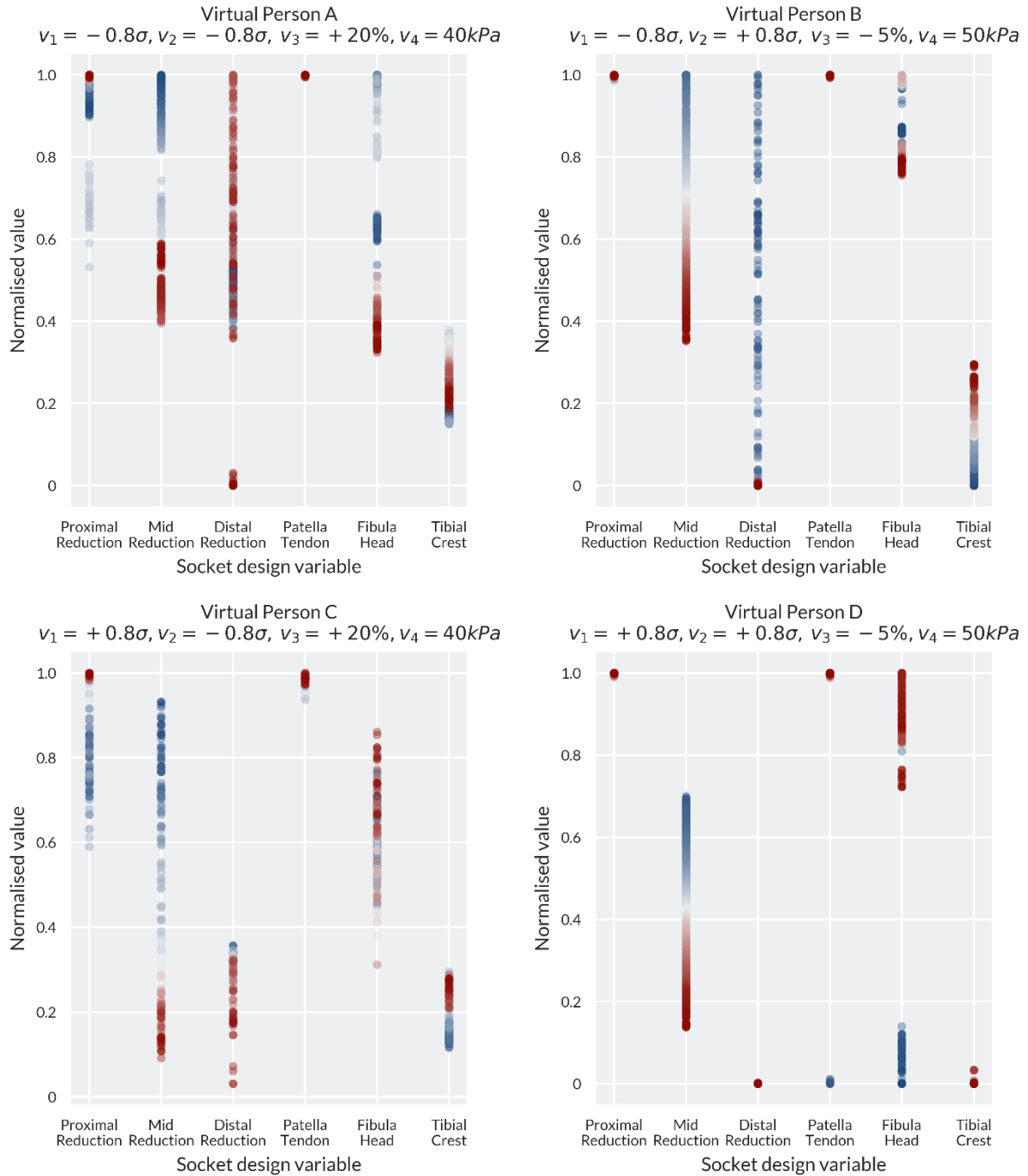
281

282

283

284

Figure 4: Optimal socket designs and corresponding predicted pressure maps for the four different virtual people at the two ends of the POF, i.e. biased towards minimising distal tip loading (top) and minimising proximal bony prominence loading (bottom), and the design with no bias (centre).



285

286 *Figure 5: Comparison of how the socket design variables (see Table 2) changed between the four cases along the Pareto*
 287 *Optimal Front. Blue denotes a bias towards FF1 (distal loading) while red denotes bias towards FF2 (proximal loading).*

288 Trends in the designs can be observed between the competing fitness functions by visualising how
 289 the optimal socket designs change along the Pareto Optimal Front (Figure 5). Across all virtual
 290 people, the patella tendon bar variable converged at the constraint maximum of 6 mm for almost all
 291 of the points along the Pareto Optimal Front. The exception was in Person D, with the longest and
 292 thinnest residual limb. When the optimiser was biased towards FF1, a few designs evolved with the
 293 patella tendon bar rectification at the 0 mm lower limit. This was offset by removal of the fibula
 294 head relief to ensure that the pressure over the residuum tip is still minimised. A clear trend for all
 295 virtual people was in the mid reduction in the socket, where the press-fit decreases along the Pareto
 296 Optimal Front from FF1 (with the aim of minimising the distal loading) to FF2 (with the aim of

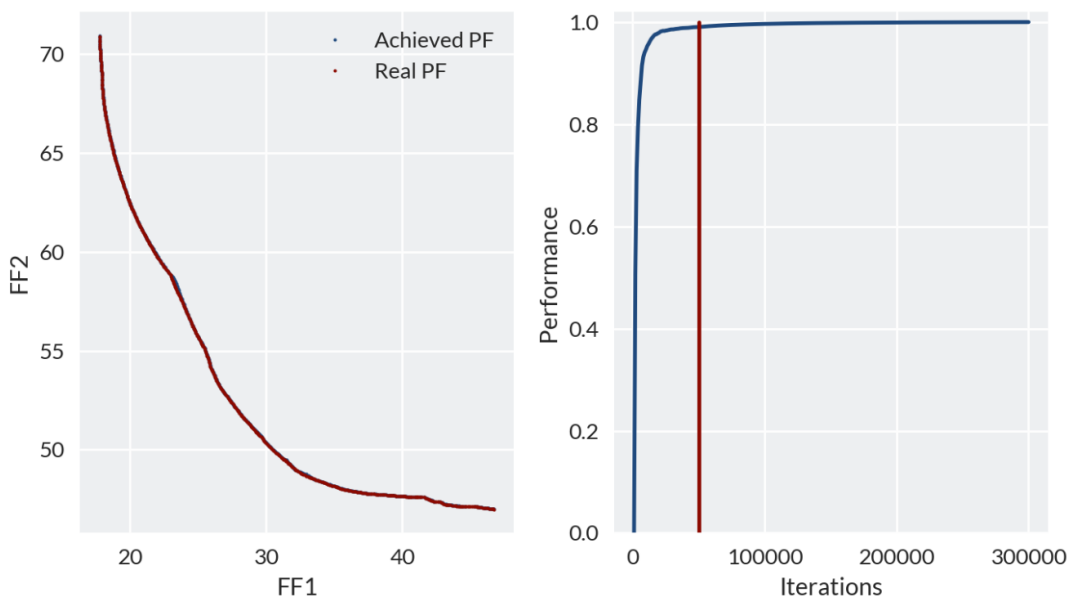
297 minimising the proximal loading). By reducing the press-fit, the pressure over the bony prominences
 298 and the peripheral shear both decreased, resulting in an increase in distal tip pressure and soft tissue
 299 strain.

300 The performance of different methodologies was evaluated using the proposed indicators, IGD and
 301 HV, and presented in the form of rankings with average values and standard deviations (Table 3). In
 302 this case the algorithms all performed in the same manner for IGD and HV. HEIA and cMLSGA were
 303 the best performing algorithms and MOEA/D and MTS performed the worst. However, the relatively
 304 similar performances of all five algorithms indicates that the complexity of the presented cases are
 305 low. The final Pareto Front was continuous and there were no constraints, which led to
 306 convergence-dominated HEIA having the best performance, over cMLSGA and NSGA-II. MOEA/D and
 307 MTS perform less well. However, this may be due to a lack of hyperparameter tuning to the
 308 particular problem. These two algorithms are dependent on a number of parameters which must be
 309 optimised for each problem, and in the present work the authors used default values described in
 310 the algorithms' original papers. The MOEA/D and MTS algorithms may perform better once tuned,
 311 now that a priori knowledge has been developed, but the present results indicate the caution with
 312 which these algorithms should be used.

313 *Table 3: Ranking of different genetic algorithms using HV and IGD as the performance indicators. * indicates if the results*
 314 *are significantly different to the next lowest rank, using the Wilcoxon's rank sum with a 0.05 confidence.*

| | | Rank | 1 | 2 | 3 | 4 | 5 |
|-----|-----------|------------|------------|------------|------------|------------|------------|
| | | Algorithm | HEIA* | cMLSGA* | NSGA-II* | MOEA/D* | MTS |
| IGD | Average | HEIA* | 0.029349 | 0.057565 | 0.1384 | 0.281601 | 0.590279 |
| | (S.D.) | | (0.001741) | (0.001553) | (0.139218) | (0.158822) | (0.049102) |
| HV | Algorithm | HEIA* | cMLSGA | NSGA-II* | MOEA/D | MTS | |
| | Average | 0.174846 | 0.174475 | 0.174461 | 0.174094 | 0.168158 | |
| | (S.D.) | (0.000027) | (0.000039) | (0.000288) | (0.000214) | (0.000464) | |

315



316

317 *Figure 6: a) The comparison of Pareto Fronts from Virtual Person 1, achieved using HEIA over 50,000 iterations ('achieved')*
 318 *and 300,000 iterations ('real'). B) The performance of HEIA over 300,000 iterations on Person 1. 0 is the starting population,*
 319 *and 1 is the best attainable set of solutions, based on the IGD values, and the red line indicates the number of function calls*
 320 *utilised in this study.*

321 In order to better understand the complexity of the problem, and to check if the best possible set of
322 solutions has been found, a set of 5 runs with 300,000 total iterations was conducted on each virtual
323 person, utilising HEIA. In this case hardly any difference was observed between 50,000 and 300,000
324 iterations. [Figure 6a](#) shows some very slightly higher uniformity and diversity of the points in the
325 high FF1 bias region with 300,000 iterations. When comparing the performance over the number of
326 generations in [Figure 6b](#), virtually no improvement in performance can be seen after 50,000
327 generations and the highest performance gain occurred before 25,000 iterations. The low possible
328 performance increase beyond 50,000 iterations in this case would not justify conducting
329 optimisation of this problem with higher values, unless the virtual person is suspected to benefit
330 from an extreme reduction in pressure over the residuum tip and the soft tissue strain around the
331 distal tibia (FF1 bias).

332 [Discussion](#)

333 This study aimed to explore a range of potential concepts for transtibial socket design using FE
334 modelling, surrogate modelling and GA-based optimisation techniques, to provide a quantitatively-
335 informed starting point for the prosthetist when designing a bespoke prosthetic socket.

336 Exploring the parametric socket design space demonstrates that biomechanical objective functions
337 are in competition, and illustrates the challenges associated with defining the 'best' socket design
338 solution. As explored in our previous work [1], by increasing the socket press fit, particularly in the
339 mid-section, an increase in longitudinal shear around the main body of the residual limb was
340 predicted. This resulted in a pressure reduction at the residuum tip coupled to a reduction in the
341 internal strain around the distal tibia. By oversizing the socket (i.e. negative press-fit) these
342 peripheral shear forces were not generated, thereby increasing the distal pressure and soft tissue
343 strain. These represent the competing fitness functions inherent in prosthetic socket design.

344 Introduction of the patella tendon bar and tibial crest rectifications provided an alternative method
345 of off-loading the residuum tip beyond a uniform press-fit. Fibula head relief is predicted to be
346 effective in reducing the high pressure that was observed over this bony prominence for the total
347 surface bearing socket designs, thus reiterating the importance of localised shape change beyond
348 applying gross scaling to the limb shape [31].

349 The sockets that emerged from the Genetic Algorithm exhibited features of both total surface
350 bearing (TSB) and patella tendon bearing (PTB) manual socket design philosophies. One consistent
351 feature along the Pareto Front for all virtual people was the patella tendon bar rectification variable,
352 which saturated at its maximum limit. This is because no optimisation cost was associated with
353 applying pressure over this region, which the Genetic Algorithm exploited to off-load the high-cost
354 residuum tip region. This effect is observed clinically for the patella tendon bearing socket where
355 prosthetists produce a marked rectification over the patella tendon to leverage its load bearing
356 capacity. Although load tolerant, there clearly would be a load threshold for injury at the patella
357 tendon, so with enhanced spatial data of load tolerance across these key residuum locations [32] an
358 additional constraint of maximal patellar tendon pressure could be included in the optimisation
359 problem.

360 Along the Pareto Front of the best solutions, trends were predicted as the bias of the optimised
361 socket varied between the two fitness functions. When fitness function 1 was dominant and the
362 Genetic Algorithm aimed to minimise pressure and soft tissue strain at the residuum tip, sockets
363 with high levels of mid-height press-fit emerged from the model. Conversely, when fitness function 2
364 was dominant and the Genetic Algorithm aimed to minimise pressure over the proximal bony

365 prominences, the global press-fit was reduced and local relief over the fibula head was increased.
366 The sockets which minimised residuum tip pressure (FF1-biased) exhibited characteristics associated
367 with a total surface bearing socket design, whilst the patella tendon bearing rectifications were
368 dominant when minimising pressure over bony prominences (FF2-biased). While it is difficult to
369 validate these findings from the current literature, a systematic review of transtibial prosthetic
370 socket designs by Safari and Meier concluded that TSB sockets exhibited improved weight-bearing,
371 greater suspension and reduced pistoning, which may be, in part, due to the increased peripheral
372 shear from the TSB socket [16]. However, extensive experimental data collection is required to
373 validate such a hypothesis.

374 Differences in the Pareto Front were observed between the virtual people. While the minimum
375 value of fitness function 1 was consistent across the cases at just below 20, the minima of fitness
376 function 2 varied substantially. This result was to be expected based upon the results of the
377 population model where residuum morphology, in particular the residuum profile, had a substantial
378 effect on the pressure over the bony prominences.

379 A range of genetic algorithms proved effective in performing multi-objective design optimisation of
380 the socket by handling the complex task of simulating the interplay between rectifications on the
381 competing objective functions of the residual limb across the presented design space. In this case
382 the performance of all methodologies was comparable and it could be concluded that the utilisation
383 of several GAs was unnecessary. However, in this case the problem is rather simple to optimise, as
384 50,000 fitness function calls are sufficient to provide good approximation of the best Pareto Front,
385 and in some cases 20,000 was adequate. The problem has continuous search and objective spaces
386 which further indicates its simplicity [33]. However, as the importance of utilising multiple
387 methodologies has been shown by previous researchers [23], it is strongly advised here to follow this
388 procedure as good practice until the design space for transtibial prosthetic sockets is better
389 understood. In the future, as more variables and objectives are added to the search space, it is
390 expected that the topology of the design space will change and therefore provide an increasing
391 challenge to resolve the optimal points, and require review of the required GA parameters and
392 convergence limits.

393 The presented multi-objective design optimisation provides an early demonstration of how the
394 speed increases achieved by surrogate techniques enable the socket design process to be framed as
395 an engineering design problem. There are several potential improvements that could be
396 implemented within this process. One such approach may be a dual-level solver where the solver
397 starts with no data, runs a full simulation on a limited population of designs, creates a surrogate
398 from these designs and evaluates the fitness of a substantially larger group across the surrogate. The
399 elite individuals, the fittest individuals in the population which are often defined as the top 10%,
400 would be retained for the next generation and the process repeated. This approach would enable
401 the GA to ignore regions which are clearly sub-optimal, and instead prioritise expensive FE analyses
402 in regions where the minima of the fitness function is more likely to be found. As an alternative
403 approach, to prevent overfitting, the surrogate might be used to generate initial generations, and
404 more expensive FE analyses used at the end to select a preferred design from the options along the
405 Pareto Front.

406 [Limitations](#)

407 User satisfaction with the socket is ultimately a subjective measure dependent upon a range of
408 human factors such as comfort, pain thresholds, and proprioception arising from a firm, functional
409 prosthesis-skeletal coupling. This means that the predictions of pressure, shear stress and soft tissue

410 strain are not directly related to comfort [34]. Furthermore, the model would not account for local
411 tissue sensitivities associated with neuromata and soft tissue injuries which could only be identified
412 in limb assessment by the prosthetist. This process might therefore be enhanced by surveying
413 functional and user-reported outcome measures across a population of socket designs.

414 No direct experimental validation of the underlying relationships between socket design and load-
415 transfer predicted by the model in this study has been performed, and such validation evidence
416 must be obtained prior to any clinical evaluation. Pressure and shear sensors [35] and lab-based
417 residuum-socket simulators [36] measure the interaction between the residual limb and socket, and
418 could be used to reinforce the findings of this study. As the model uses invented residual limb
419 shapes with thousands of socket designs, it is clearly infeasible to perform experimental validation
420 upon any more than a limited subset of data points in this model. However, in future, a limited
421 number of key socket designs should be tested to validate the conclusions of this model.
422 Furthermore, the population-based surrogate model only characterises a simplified representation
423 of the variability which exists across the population. As discussed previously [1], a practical
424 application of these tools requires further data to construct the surrogate model, for example
425 variation in femoral or patella geometry, bone and liner material properties, as well as dynamic load
426 cases. Some confidence is provided by corroboration with literature reports of pressure predictions
427 across the limb between 30-100 kPa during gait for TSB sockets [37-40] and 25-320 kPa for PTB [40-
428 42], which is consistent with the range of predicted pressures for the FF1-biased sockets in this
429 study.

430 As the study is an initial investigation into the methods and potential it forms the basis for further
431 investigations that provide a more complex design. In increasing this complexity a number of
432 elements will change. First, the kriging model itself will become more complex providing some
433 challenges in the use of this model which must be investigated. Second, the design space will change
434 and this will provide a different set of optimisation challenges. In both instances the methods used
435 will need to be evaluated carefully. In the case of more complex design spaces, other surrogates
436 might become more appropriate, such as Deep Reinforcement learners. These are subject to a
437 disadvantage of requiring more input data. For the optimisation, it is likely that the space will
438 become more discontinuous [43], similar to other more complex applications, and this will require
439 algorithms with stronger diversity [23]: NSGA-II and cMLSGA. There is also likely to be a greater
440 separation between specialist, which will have even further reduced performance compared to the
441 general solvers: NSGA-II, cMLSGA and HEIA.

442 Clinical applications

443 Attempting to use simulations to inform clinical decision-making requires extreme caution,
444 especially when applied to devices which depend upon personalised design to ensure comfort and
445 functional efficacy, as comfort and proprioception are difficult to quantify. Crucially, in prosthetic
446 limb design we would argue that these techniques should not be used in isolation, or substituted for
447 human-facing clinical practice. The expert prosthetist must retain control over socket design, and the
448 presented optimisation approach could be used to provide a 'first-guess' rectification map. The
449 prosthetist would then modify this design according to their own clinical reasoning which combines
450 palpation, user feedback and re-evaluation. Other technologies such as real-time pressure
451 measurements and predictions from the previously reported PCA-Kriging model [1], incorporated
452 with their skill and experience could provide a technology-enhanced limb assessment. This approach
453 will help the community to test the key translational research question in this field: can the clinical

454 application of FEA support the prosthetist's evidence-base and enable delivery of comfortable,
455 highly functional prosthetic limbs to users in a more timely and efficient manner?

456 Conclusion

457 This paper provides a first assessment of the use of multi-objective optimisation in the design of
458 prosthetic socket design. The experiential judgement and skill-based process of prosthetic socket
459 design is framed as a multi-objective engineering design problem. This is achieved by developing
460 parametric models of the residual limb informed by statistical shape modelling techniques and the
461 prosthetic socket incorporating both total surface bearing and patella tendon bearing rectifications,
462 which allow the underlying biomechanical relationships between the residual limb and prosthetic
463 socket to be predicted. In line with experimental data to allow detailed biomechanical validation, the
464 developed methods show substantial potential to be used as part of a more informed socket design
465 process, and provide clinicians with support for selecting from the range of candidate design
466 approaches. The resulting designs replicate the general forms of the two most popular designs:
467 patella tendon bearing and total surface bearing sockets, at the extremes with a series of variations
468 that result in designs that are a compromise between both in the centre. This results in a difference
469 in pressure of up to 31 kPa over the fibula head and 14 kPa over the residuum tip.

470 Acknowledgments

471 Funding: The authors would like to thank the following for their financial support: JWS: the
472 University of Southampton's EPSRC Doctoral Training Program (ref EP/M508147/1); PRW: the
473 EPSRC-NIHR "Medical Device and Vulnerable Skin Network" (ref EP/M000303/1 & EP/N02723X/1);
474 ASD: the Royal Academy of Engineering, UK, (ref RF/130). We thank Herbert Ganter and the other
475 members of the ImpAmp consortium under EUROTARS project (ref 9396) for technical support and
476 data collection.

477 Data availability: Supporting data are openly available from the University of Southampton
478 repository at <http://dx.doi.org/10.5258/SOTON/XXXXX <-- TO BE ASSIGNED AND ACTIVATED ON>
479 ACCEPTANCE

480 **References**

481 [1] J. W. Steer, M. Browne, P. R. Worsley, and A. S. Dickinson, "Predictive prosthetic socket design. Part 1:
482 population-based evaluation of transtibial prosthetic sockets by FEA-driven surrogate modelling,"
483 *Biomech. Model. Mechanobiol.*, 2019.

484 [2] A. Eklund and S. Sexton, "WHO standards for prosthetics and orthotics," 2017.

485 [3] M. Kerr, G. Rayman, and W. J. Jeffcoate, "Cost of diabetic foot disease to the National Health Service
486 in England," *Diabet. Med.*, vol. 31, no. 12, pp. 1498–1504, 2014.

487 [4] J. C. H. Goh, P. V. S. Lee, S. L. Toh, and C. K. Ooi, "Development of an integrated CAD-FEA process for
488 below-knee prosthetic sockets," *Clin. Biomech.*, vol. 20, no. 6, pp. 623–629, 2005.

489 [5] G. Colombo, G. Facoetti, D. Regazzoni, and C. Rizzi, "A full virtual approach to design and test lower
490 limb prosthesis," *Virtual Phys. Prototyp.*, vol. 8, no. 2, pp. 97–111, 2013.

491 [6] C. W. Radcliffe, "The Biomechanics of Below-Knee Prostheses in Normal, Level, Bipedal Walking," *Artif
492 Limbs*, vol. 6, pp. 16–24, 1962.

493 [7] G. G. Kuhn, "Kondylen Bettung Münster am Unterschenkel-Stumpf 'KBM-Prothese,'" *Atlas
494 d'Appareillage Proth{é}tique et Orthop{é}dique*, no. 14, 1966.

495 [8] G. Murdoch, "The 'Dundee' Socket—A Total Contact Socket for the Below-Knee Amputation," no. 4,
496 1964.

497 [9] J. C. H. Goh, P. V. S. Lee, and S. Y. Chong, "Stump/socket pressure profiles of the pressure cast
498 prosthetic socket," *Clin. Biomech.*, vol. 18, no. 3, pp. 237–243, 2003.

499 [10] S. Laing, P. V. S. Lee, J. Lavranos, and N. Lythgo, "The functional, spatio-temporal and satisfaction
500 outcomes of transtibial amputees with a hydrocast socket following an extended usage period in an
501 under-resourced environment," *Gait Posture*, vol. 66, no. July, pp. 88–93, 2018.

502 [11] J. C. H. Goh, P. V. S. Lee, and S. Y. Chong, "Comparative study between patellar-tendon-bearing and
503 pressure cast prosthetic sockets," *J. Rehabil. Res. Dev.*, vol. 41, no. 3, pp. 491–501, 2004.

504 [12] S. Laing, N. Lythgo, J. Lavranos, and P. V. S. Lee, "Transtibial Prosthetic Socket Shape in a Developing
505 Country: A study to compare initial outcomes in Pressure Cast hydrostatic and Patella Tendon Bearing
506 designs," *Gait Posture*, vol. 58, no. July, pp. 363–368, 2017.

507 [13] P. Lee, J. Goh, and S. Cheung, "Biomechanical evaluation of the pressure cast (PCast) prosthetic socket
508 for transtibial amputee," in *Proceedings of the World Congress on Medical Physics & Biomedical
509 Engineering*, 2000.

510 [14] T. Staats and J. Lundt, "The UCLA total surface bearing suction below-knee prosthesis," *Clin Prosthet
511 Orthot*, vol. 11, no. 3, pp. 118–130, 1987.

512 [15] K. Hachisuka, K. Dozono, H. Ogata, S. Ohmine, H. Shitama, and K. Shinkoda, "Total surface bearing
513 below-knee prosthesis: Advantages, disadvantages, and clinical implications," *Arch. Phys. Med.
514 Rehabil.*, vol. 79, no. 7, pp. 783–789, 1998.

515 [16] M. R. Safari and M. R. Meier, "Systematic review of effects of current transtibial prosthetic socket
516 designs—Part 2: Quantitative outcomes," *J. Rehabil. Res. Dev.*, vol. 52, no. 5, pp. 509–526, 2015.

517 [17] M. R. Safari and M. R. Meier, "Systematic review of effects of current transtibial prosthetic socket
518 designs—Part 1: Qualitative outcomes," *J. Rehabil. Res. Dev.*, vol. 52, no. 5, pp. 491–508, 2015.

519 [18] A. Palevski, I. Glaich, S. Portnoy, E. Linder-Ganz, and A. Gefen, "Stress Relaxation of Porcine Gluteus
520 Muscle Subjected to Sudden Transverse Deformation as Related to Pressure Sore Modeling," *J.
521 Biomech. Eng.*, vol. 128, no. 5, p. 782, 2006.

522 [19] S. Portnoy, I. Siev-Ner, Z. Yizhar, a. Kristal, N. Shabshin, and a. Gefen, "Surgical and morphological
 523 factors that affect internal mechanical loads in soft tissues of the transtibial residuum," *Ann. Biomed.*
 524 *Eng.*, vol. 37, no. 12, pp. 2583–2605, 2009.

525 [20] K. Hoyt, T. Kneezel, B. Castaneda, and K. J. Parker, "Quantitative sonoelastography for the in vivo
 526 assessment of skeletal muscle viscoelasticity," *Phys. Med. Biol.*, vol. 53, no. 15, pp. 4063–4080, 2008.

527 [21] D. E. Goldberg and J. H. Holland, "Genetic algorithms and machine learning," *Mach. Learn.*, vol. 3, no.
 528 2, pp. 95–99, 1988.

529 [22] D. H. Wolpert and W. G. Macready, "No Free Lunch Theorems for Optimization 1 Introduction," *IEEE*
 530 *Trans. Evol. Comput.*, vol. 1, no. 1, pp. 67–82, 1997.

531 [23] Z. Wang, J. Bai, A. Sobey, J. Xiong, and A. Shenoi, "Optimal design of triaxial weave fabric composites
 532 under tension," *Compos. Struct.*, vol. 201, no. June, pp. 616–624, 2018.

533 [24] K. Deb, A. Pratap, S. Agarwal, and T. Meyarivan, "A fast and elitist multiobjective genetic algorithm:
 534 NSGA-II," *IEEE Trans. Evol. Comput.*, vol. 6, no. 2, pp. 182–197, 2002.

535 [25] Q. Zhang and H. Li, "MOEA/D: A multiobjective evolutionary algorithm based on decomposition," *IEEE*
 536 *Trans. Evol. Comput.*, vol. 11, no. 6, pp. 712–731, 2007.

537 [26] L. Y. Tseng and C. Chen, "Multiple trajectory search for multiobjective optimization," in *2007 IEEE*
 538 *Congress on Evolutionary Computation, CEC 2007*, 2007, vol. 758, pp. 3609–3616.

539 [27] Q. Lin et al., "A hybrid evolutionary immune algorithm for multiobjective optimization problems," *IEEE*
 540 *Trans. Evol. Comput.*, vol. 20, no. 5, pp. 711–729, 2016.

541 [28] P. A. Grudniewski and A. J. Sobey, "cMLSGA: co-evolutionary Multi-Level Selection Genetic
 542 Algorithm," *Swarm Evol. Comput. Under Rev.*

543 [29] P. A. Grudniewski and A. J. Sobey, "Behaviour of Multi-Level Selection Genetic Algorithm (MLSGA)
 544 using different individual-level selection mechanisms," *Swarm Evol. Comput.*, pp. 1–29, 2018.

545 [30] M. Li and X. I. N. Yao, "Quality Evaluation of Solution Sets in Multiobjective Optimisation : A Survey,"
 546 vol. 1, no. 1, pp. 1–43, 2018.

547 [31] J. C. H. Goh, P. V. S. Lee, and S. Y. Chong, "Static and dynamic pressure profiles of a patellar-tendon-
 548 bearing (PTB) socket.," *Proc. Inst. Mech. Eng. H.*, vol. 217, no. 2, pp. 121–6, 2003.

549 [32] J. L. Bramley, P. R. Worsley, L. Bostan, D. L. Bader, and A. S. Dickinson, "Investigating the Effects of
 550 Simulated Prosthetic Loading on Intact and Trans-Tibial Residual Limb Dermal Tissues," *Prosthetics &*
 551 *Orthotics Intl.*, vol. 43, Suppl. 1, 2019.

552 [33] Y. G. Woldesenbet, G. G. Yen, and B. G. Tessema, "Constraint Handling in Multiobjective Evolutionary
 553 Optimization," *IEEE Trans. Evol. Comput.*, vol. 13, no. 3, pp. 3077–3084, 2009.

554 [34] A. F. Mak, M. Zhang, and D. A. Boone, "State-of-the-art research in lower-limb prosthetic
 555 biomechanics-socket interface: a review.," *J. Rehabil. Res. Dev.*, vol. 38, no. 2, pp. 161–174, 2001.

556 [35] P. Laszczak, L. Jiang, D. L. Bader, D. Moser, and S. Zahedi, "Development and validation of a 3D-printed
 557 interfacial stress sensor for prosthetic applications.," *Med. Eng. Phys.*, vol. 37, no. 1, pp. 132–7, 2015.

558 [36] M. P. McGrath et al., "Development of a residuum/socket interface simulator for lower limb
 559 prosthetics," *Proc. Inst. Mech. Eng. Part H J. Eng. Med.*, vol. 231, no. 3, p. 095441191769076, 2017.

560 [37] E. A. Al-Fakih, N. A. A. Osman, A. Eshraghi, and F. R. M. Adikan, "The capability of fiber Bragg grating
 561 sensors to measure amputees??? trans-tibial stump/socket interface pressures," *Sensors*
 562 (Switzerland), vol. 13, no. 8, pp. 10348–10357, 2013.

563 [38] T. L. Beil, G. M. Street, and S. J. Covey, "Interface pressures during ambulation using suction and
564 vacuum-assisted prosthetic sockets.,," *J. Rehabil. Res. Dev.*, vol. 39, no. 6, pp. 693–700, 2002.

565 [39] T. L. Beil and G. M. Street, "Comparison of interface pressures with pin and suction suspension
566 systems.,," *J. Rehabil. Res. Dev.*, vol. 41, no. 6A, pp. 821–828, 2004.

567 [40] T. Dumbleton et al., "Dynamic interface pressure distributions of two transtibial prosthetic socket
568 concepts," *J. Rehabil. Res. Dev.*, vol. 46, no. 3, pp. 405–415, 2009.

569 [41] M. Zhang, a R. Turner-Smith, a Tanner, and V. C. Roberts, "Clinical investigation of the pressure and
570 shear stress on the trans-tibial stump with a prosthesis.,," *Med. Eng. Phys.*, vol. 20, no. 3, pp. 188–198,
571 1998.

572 [42] P. Dou, X. Jia, S. Suo, R. Wang, and M. Zhang, "Pressure distribution at the stump/socket interface in
573 transtibial amputees during walking on stairs, slope and non-flat road," *Clin. Biomech.*, vol. 21, no. 10,
574 pp. 1067–1073, 2006.

575 [43] A. Sobey, J. Blanchard, P. Grudniewski, and T. Savasta, "There's no free lunch: A study of Genetic
576 Algorithm use in Maritime Applications," in *Conference on Computer Applications and Information
577 Technology in the Maritime Industries*, 2019.

578